20122001 3A (3/3)

厚生労働科学研究費補助金

第３次対がん総合戦略研究事業

# がん化学予防剤の開発に関する基礎及び臨床研究

平成２４年度　総括・分担研究報告書

（３／３）

研究代表者　武藤　倫弘

Osaka City Med. J. Vol. 58, 13-24, 2012

# AGR2 as a Potential Biomarker of Human Lung Adenocarcinoma

KYUKWANG CHUNG[1,2], NORITOSHI NISHIYAMA[1], HIDEKI WANIBUCHI[2], SHOTARO YAMANO[2], SHOJI HANADA[1,2], MIN WEI[2], SHIGEFUMI SUEHIRO[1], and ANNA KAKEHASHI[2]

*Departments of Thoracic Surgery[1] and Pathology[2], Osaka City University, Graduate School of Medicine*

## Abstract

***Background***

The present study aimed to identify useful candidate biomarkers of lung adenocarcinoma for clinical diagnosis and treatment using proteomics technology.

***Methods***

We assessed frequently highly overexpressed proteins in 12 cases of lung adenocarcinoma compared with adjacent normal tissue samples by liquid chromatography tandem mass spectrometry (LC-MS/MS) coupled with isobaric tags for relative and absolute quantitation (iTRAQ) technology, and validated the expression of target proteins by immunohistochemistry in 268 lung adenocarcinoma cases. Protein expression and clinicopathological variables were compared statistically for the evaluation of novel biomarkers.

***Results***

One hundred seventy-seven proteins displaying significant quantitative changes compared with adjacent normal-appearing lung tissue were identified in more than 9 out of 12 lung adenocarcinoma patients. Based on the results of liquid chromatography tandem mass spectrometry, Ingenuity Pathway, and immunohistochemical analyses, anterior gradient homolog 2 (AGR2) (upregulated 9.9-fold) was selected as a potential biomarker of human lung adenocarcinoma. AGR2 was positive in 94% of lung adenocarcinoma patients. Negative AGR2 expression was associated with poor survival (p=0.007).

***Conclusions***

AGR2 is likely to become a biomarker for clinical applications.

Key Words: Proteomics; Lung adenocarcinoma; AGR2; Prognostic biomarker

## Introduction

Lung cancer is the leading cause of cancer-related mortality, with an increasing incidence in Japan and worldwide. Despite advances in early diagnostic methods and treatment modalities,

Received October 11, 2011; accepted November 29, 2011.
Correspondence to: Hideki Wanibuchi, MD.
Department of Pathology, Osaka City University, Graduate School of Medicine,
1-4-3 Asahimachi, Abeno-ku, Osaka 545-8585, Japan
Tel: +81-6-6645-3735; Fax: +81-6-6646-3093
E-mail: wani@med.osaka-cu.ac.jp

lung cancer is often diagnosed at an advanced stage and presents a poor prognosis. Early detection and complete surgical resection still remains the most successful curative therapeutic option. Non-small cell lung cancer (NSCLC) is a heterogeneous group and can be subdivided into three main histological subtypes: adenocarcinoma, squamous cell carcinoma, and large cell carcinoma, and adenocarcinomas are now the most common type of lung cancer. The TNM classification is the most important predictor of survival in NSCLC; however, occasionally patients staged according to the TNM classification have different survival times[1]. Thus, novel prognostic markers, such as ones that identify the subgroup of patients with a high risk of recurrence, are needed for better therapy design. Additionally, in early detection, the commonly available serum markers such as CEA, CA19-9, SCC, CYFRA21-1, NSE, and ProGRP have limited sensitivity and specificity[2]. Therefore, new candidate biomarkers for lung cancer have been sought in the hope of achieving early detection of the disease, improving diagnosis, predicting response, or monitoring recurrence after treatment. Although many candidate biomarkers for the management of patients with NSCLC have been proposed, larger prospective trials to validate them have not been undertaken and their clinical usefulness remains limited at present[3]. The discovery of new potential biomarkers is difficult because of the high degree of heterogeneity of NSCLC.

Proteomics can be defined as the comprehensive analysis of the proteome, which is composed of vital protein parts of a living organism. The development of accurate mass spectrometry, advances in of ionization technology, progression of powerful computing and completion of the human genome sequence have accelerated proteomics enormously in recent years. Beyond genomics, the next major challenge is the identification of novel proteins and to understand the structure, function, and interactions of proteins and other molecules. The main aim of clinical proteomics in the field of oncology is the discovery of novel diagnostic, prognostic, or therapeutic markers for future individualized therapy. With recent advances in mass spectrometry techniques, it is now possible to investigate protein expression profiles from biological specimens, healthy and diseased, over a wide range of molecular weights. Their relative expression abundances can even be quantified. Recently, isobaric tags for relative and absolute quantitation (iTRAQ™) reagents have been introduced (AB Sciex, Framingham, USA). The iTRAQ technology allows multiplexed relative quantitative proteomic analysis under the same experimental conditions and, in combination with liquid chromatography tandem mass spectrometry (LC-MS/MS) techniques, increases analytical accuracy and precision. Accordingly, the technology facilitates identification of markers with high selectivity, sensitivity, and specificity[4]. Accordingly, we recently demonstrated significant overexpression of novel biomarkers in rat and mouse liver preneoplastic lesions, which drive their transformation into hepatocellular carcinomas, using the QSTAR Elite LC-MS/MS system allowing multiple protein identification[5,6].

The aim of this study was to identify candidate biomarkers of lung adenocarcinoma in comparison with adjacent normal lung tissue samples, using proteomics coupled with iTRAQ technology. We also aimed to validate the candidates with immunohistochemical staining and identify correlations between the expression of the candidates and clinicopathological variables, thus identifying useful biomarkers for clinical diagnosis and treatment.

## Methods

### *Institutional review board approval and informed consent*

This study was approved by the ethics committee at Osaka City University Graduate School of Medicine. Written informed consent was received from all patients.

### *Patients and tissue samples*

Patients were 268 cases with primary lung adenocarcinoma resected at Osaka City University Hospital from January 2004 to December 2008 who had no systemic chemotherapy before tumor resection. Diagnoses were performed by pathologists from the pathology department in our hospital according to the criteria of the World Health Organization and were staged according to the TNM classification of the International Union Against Cancer. The mean age at the time of surgery was 67 years (range: 20 to 93 years) and the median postoperative observation time was 24 months (range: 3 to 61 months). Clinical follow-up data, including disease-specific survival, were recorded from the day of surgery to the time of death or to the last follow-up observation. All lung tumors and adjacent normal lung tissue were obtained at the time of surgery, frozen immediately in liquid nitrogen, and stored at −80℃ until analysis.

### *LC-MS/MS analysis*

Twelve cases were selected randomly among the subjects. The lung tumor and adjacent normal tissue samples of the 12 cases (20 mg each) were homogenized and dissolved in 500 μL of 9 M Urea, 2% CHAPS lysis buffer with protease inhibitors. In addition, the cell lysate was then treated by ultrasonication. After acetone precipitation, protein concentrations were measured by the BCA Protein Assay (Pierce, IL, USA). Reduction, alkylation, digestion, and subsequent peptide labeling of 50 μg protein for each sample were performed using the AB Sciex iTRAQ Reagent Multi-Plex Kit (AB Sciex, Concord, ON, Canada). The adjacent normal and lung tumor tissues of one subject were labeled with the iTRAQ 114 and 115 Da signature ion signal reagents, respectively, and in the same way, the adjacent normal and lung tumor tissues of another subject were labeled with 116 and 117 Da ion signals in MS/MS mode. The iTRAQ-labeled samples were loaded onto an ICAT cation exchange cartridge (AB Sciex). The peptides were eluted as eight fractions (1 mL KCl solution of 10, 30, 50, 70, 90, 110, and 200 mM) and the supernatant was evaporated in a vacuum centrifuge. Peptides of each faction were resuspended in 500 μL of solvent A (98% water/2% ACN/0.1% formic acid, v/v) and injected into Sep-Pak Light C18 cartridges (Waters Corporation, Milford, MA, USA). A double elution was performed with 1.5 mL of solvent A and B (30% water/70% ACN/0.1% formic acid, v/v) for desalting and concentrating. The supernatant was evaporated in a vacuum centrifuge and resuspended in 20 μL of 0.1% formic acid. Proteome analysis was performed on a DiNa-AI nano LC System (KYA Technologies, Tokyo, Japan) coupled to a QSTAR Elite Hybrid mass spectrometer (AB Sciex, Concord, ON, Canada) through a NanoSpray ion source (AB Sciex, Concord, ON, Canada). The separation of samples was performed isocratically (95(A)/5(B), v/v). A 5-μL injection loop was manufactured in-house by measuring an appropriate length of fused-silica capillary (32.0 cm, 30 μm id), and full loop injection was achieved by total injection of 5 μL via a six-port switching CN2 valve injector (KYA Technologies, Tokyo, Japan). The pump output (5 μL/min) was split before the injection port to a flow rate of 200 nL/min. The column effluent enters the spray chamber through a tapered stainless steel emitter and is directly electrosprayed into QSTAR System ion trap mass spectrometer in the positive mode for nanoESI-MS/MS analysis. The emitter position

was adjusted under a microscope and positioned in front of the orifice at a distance of 1.5 mm. Ion spray voltage was set between 1400 and 1600 V to achieve a stable current. Heated nitrogen drying gas (3.0 L/min, 200℃) was introduced into the spray chamber to aid in desolvation. No nebulizing gas was employed. Source voltage was adjusted such that the precursor ion generated maximized product ion signal from the tandem experiment. Each sample was run for 150 min.

MS/MS data were searched against the Swiss Protein database (HUMAN) using ProteinPilot™ software (version 2.0, AB Sciex, Concord, ON, Canada) with trypsin set as the digestion enzyme and methyl methanethiosulfonate as the cysteine modification. The search results were further processed by ProteinPilot™ software using the Paragon Algorithm for removal of redundant hits and comparative quantitation, resulting in the minimal set of justifiable identified proteins. All reported data were used at 95% confidence cut-off limit. Relative quantitation of peptides was calculated as a ratio by dividing the iTRAQ reporter intensity at 115.0, 117.0, m/z (lung tumor) by that at 114.0, and 117.0 m/z (adjacent normal tissue). The ratios of peptides that support the existence of one protein were averaged for protein relative quantitation. After the one simple t-test of averaged protein ratio against 1 to assess the validity of the protein expression changes, a p-value was reported. Protein ratios with a p-value less than 0.05 were considered reliable. Previously standard deviations of the protein ratio, which stem from technical variation, were reported to be less than 0.3 in 90% of iTRAQ experimental runs[7]. Therefore, expression changes greater than 1.6-fold or less than 0.625-fold of normalized expression levels were considered to be outside the range of technical variability.

***Selection of candidate proteins for biomarkers and validation by immunohistochemistry***

Proteins highly and frequently overexpressed in tumor tissue were noted as candidate biomarkers associated with lung adenocarcinoma. Immunohistochemical staining was performed by the ABC method using a primary rabbit monoclonal anterior gradient homolog 2 (AGR2) (clone ab76473, Abcam) primary antibody. After deparaffinization, gradual dehydration, and antigen retrieval, the endogenous peroxidase activity was blocked. The first antibody (diluted 1:1000 in 1.5% goat serum in PBS) was applied at 4℃ overnight. A biotinylated goat anti-rabbit IgG (diluted 1:200 in 1.5% goat serum in PBS) was applied as secondary antibody for 30 min, and avidin-biotin peroxidase complex was applied for 30 min. The peroxidase reaction was developed using 3,3-diaminobenzidine tetrahydrochloride (DAB) and hydrogen peroxide in Tris-buffered saline for 2 min. Hematoxylin was used for counterstaining. The immunostains were examined by two independent pathologists who analyzed clinicopathological data under the light microscope. Cells showing cytoplasmic staining were evaluated as positive. The staining for AGR2 was classified into three categories according to the percentage of carcinoma cells positive for AGR2: staining in >50% of tumor cells, strongly positive (scored as 2+); staining in 1 to 50% of tumor cells, weakly positive (1+); and staining in <1% of tumor cells, negative (0).

***Statistical analysis***

Statistical analysis was carried out using SPSS, version 17.0. Statistical significance of the associations between expression of AGR2 and various clinicopathological variables was evaluated using Fisher's exact and chi-square tests. Survival curves were calculated from the day of surgery to the relapse of death or to the last follow-up observation using the Kaplan-Meier

method, and differences in survival curves were assessed with the log-rank test. Multivariate analyses were calculated according to the Cox regression model to determine associations between clinicopathological variables and disease-specific mortality. P value $<0.05$ was considered statistically significant.

## Results

### *LC-MS/MS analysis*

After the labeling procedure and nano-LC-separation, derivatized peptides were identified and quantified by MS/MS analysis with QSTAR Elite hybrid mass spectrometer and iTRAQ reagents. Each sample was run twice and, in 12 measurements, the mean number of identified proteins in both runs was 256 (≧95% confidence, $p<0.05$). The LC-MS/MS and ProteinPilot analyses results of 12 patients were averaged and further analyzed by Ingenuity Pathway Analysis (IPA). The results are presented in Figure 1. Most of the proteins were overexpressed in the cytoplasm of tumor cells (Fig. 1A). One hundred seventy-seven proteins displaying significant quantitative changes compared with adjacent normal-appearing lung tissue were identified in lung adenocarcinomas of more than 9 patients out of 12 patients. These proteins

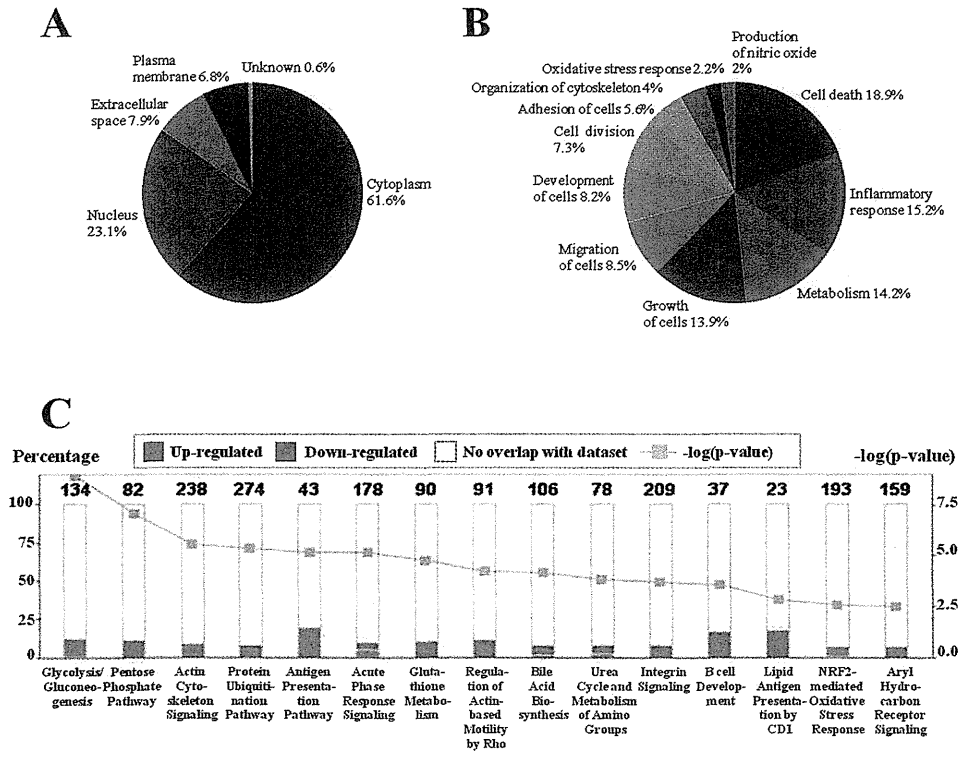


**Figure 1.** Ingenuity Pathway Analysis for alterations to protein expression in human lung adenocarcinomas of 12 patients. localization (A), biological process (B), and canonical pathways of identified proteins (C). All differentially identified proteins (100%) in lung adenocarcinoma were subdivided according to the localization and biological process as indicated by Ingenuity Pathway Analysis. The numbers of proteins for each localization and biological process were expressed as percentages. In Figure 1C, all differentially expressed proteins in lung adenocarcinoma were subdivided according to their participation in Canonical pathways as indicated by Ingenuity Pathways Analysis. In Figure 1C numbers of proteins with altered expression are represented as (−log (p value)). P value is calculated automatically by the Ingenuity Pathway Analysis based on the statistical analysis of the number of proteins participating in canonical pathways. No overlap with dataset means the number of proteins which were not implicated in canonical pathways.

**Table 1. Proteins overexpressed in the lung adenocarcinomas of 12 patients**

| Protein name (symbol) | GI number | No. cases | Location | Type | Function | Fold change |
|---|---|---|---|---|---|---|
| anterior gradient homolog 2 (Xenopus laevis) (AGR2) | 67462105 | 9 | ES, C | Other | MS | 9.9 |
| prothymosin, alpha (PTMA) | 135834 | 12 | N | Other | TR | 4.5 |
| enolase 1, (alpha) (ENO) | 119339 | 12 | C | TR | TR | 4.2 |
| non-metastatic cells 2, protein (NM23B) (NME2) | 127983 | 12 | N | K | TR, NM | 3.6 |
| interleukin enhancer binding factor 3, 90kDa (ILF3) | 62512150 | 9 | N, C | TR | TR | 2.9 |
| signal transducer and activator of transcription 1, 91kDa (STAT1) | 2507413 | 9 | N | TR | TR | 3.2 |
| RNA binding motif protein, X-linked (RBMX) | 23503093 | 9 | N | Other | RNA S | 3.8 |
| synaptotagmin binding, cytoplasmic RNA interacting protein (SYNCRIP) | 92090361 | 11 | N, C | Other | RNA S-P | 2.6 |
| heterogeneous nuclear ribonucleoprotein L (HNRNPL) | 133274 | 9 | N, C | Other | RNA S-P | 2.7 |
| DEAD (Asp-Glu-Ala-Asp) box polypeptide 39A (DDX39A) | 61212932 | 11 | N | E | RNA S | 2.9 |
| DEAD (Asp-Glu-Ala-Asp) box polypeptide 3, X-linked (DDX3X) | 3023628 | 9 | C, N | E | RNA B | 2.9 |
| acidic (leucine-rich) nuclear phosphoprotein 32 family, member A (ANP32A) | 730318 | 10 | N, C | Other | T, RNA M | 3.5 |
| high-mobility group box 3 (HMGB3) | 85701353 | 9 | N | Other | DNA REP | 10.6 |
| parathymosin (PTMS) | 135846 | 9 | N, C | Other | DNA REP | 2.8 |
| splicing factor proline/glutamine-rich (SFPQ) | 1709851 | 10 | N, C | Other | DNA RR, TR | 3.1 |
| nucleophosmin (nucleolar phosphoprotein B23, numatrin) (NPM1) | 114762 | 12 | N | TR | DNA RR, ST | 3.9 |
| non-POU domain containing, octamer-binding (NONO) | 67460768 | 10 | C, N | Other | DNA RR, TR | 3.3 |
| ribosome binding protein 1 homolog 180kDa (dog) (RRBP1) | 23822112 | 11 | C | T | TRL | 4.9 |
| Tu translation elongation factor, mitochondrial (TUFM) | 1706611 | 9 | C | TR | TRL | 3.0 |
| CNDP dipeptidase 2 (metallopeptidase M20 family) (CNDP2) | 23396498 | 9 | C | P | PRO, M | 2.6 |
| leucine aminopeptidase 3 (LAP3) | 124028615 | 11 | C | P | PRO | 3.0 |
| coatomer protein complex, subunit alpha (COPA) | 1705996 | 11 | C | T | PT | 4.3 |
| thioredoxin domain containing 5 (endoplasmic reticulum) (TXNDC5) | 29839560 | 10 | C | E | T, AAP | 4.1 |
| coatomer protein complex, subunit gamma (COPG) | 12229771 | 9 | C | T | PT | 3.2 |
| archain 1 (ARCN1) | 1351970 | 10 | C, GA | Other | PT | 3.9 |
| cofilin 1 (non-muscle) (CFL1) | 116848 | 12 | N, C | Other | CS, ACS | 3.1 |
| tropomyosin 4 (TPM4) | 54039746 | 12 | C | Other | CS, ACS | 2.6 |
| coronin, actin binding protein, 1A (CORO1A) | 1706004 | 11 | C, IS | Other | CS, ACS | 2.6 |
| plectin (PLEC) | 134044255 | 11 | C | Other | CS, ACS | 2.5 |
| capping protein (actin filament) muscle Z-line, alpha 1 (CAPZA1) | 1705650 | 9 | C | Other | CS, ACS | 2.9 |
| coactosin-like 1 (Dictyostelium) (COTL1) | 21759076 | 9 | C | Other | CS, ACS | 2.5 |
| fascin homolog 1, actin-bundling protein (FSCN1) | 2498357 | 10 | C | Other | CS, ACS | 2.8 |
| myosin, heavy chain 9, non-muscle (MYH9) | 6166599 | 12 | C | E | CS | 2.6 |
| keratin 8 (KRT8) | 90110027 | 12 | C | Other | CS | 3.5 |
| keratin 18 (KRT18) | 125083 | 12 | C | Other | CS | 2.8 |
| keratin 19 (KRT19) | 90111766 | 10 | C | Other | CS | 2.8 |
| microtubule-associated protein 4 (MAP4) | 20455500 | 12 | C | Other | CS | 2.6 |
| tubulin, beta 6 (TUBB6) | 68776070 | 11 | C | Other | CS | 2.7 |
| caldesmon 1 (CALD1) | 2498204 | 10 | C | Other | CS | 2.8 |
| transgelin 2 (TAGLN2) | 586000 | 12 | PM, C | Other | CS | 3.1 |
| cytoskeleton-associated protein 4 (CKAP4) | 74735614 | 10 | C | Other | Unknown | 3.6 |
| S100 calcium binding protein A11 (S100A11) | 1710818 | 12 | C | Other | ST | 5.1 |
| S100 calcium binding protein A6 (S100A6) | 116509 | 11 | C | T | ST, AXO | 3.3 |
| ras-related C3 botulinum toxin substrate 2 (rho family) (RAC2) | 131806 | 9 | C | E | ST, ACS | 2.6 |
| IQ motif containing GTPase activating protein 1 (IQGAP1) | 1170586 | 10 | C | Other | ST, ACS | 2.5 |
| thymidine phosphorylase (TYMP) | 67477361 | 10 | ES, C | GR | NM, ANG | 2.7 |
| periostin, osteoblast specific factor (POSTN) | 93138709 | 9 | ES, C | Other | A, MIG, I | 4.0 |

Localization: C, cytoplasm; N, nucleus; PM, plasma membrane; ES, extracellular space; GA, Golgi apparatus; and IS, immunological synapse.

Type: E, enzyme; K, kinase; T, transporter; TR, transcription regulator; GR, growth regulator; and P, peptidase.

Function: CS, cytoskeleton; ACS, actin cytoskeleton; M, metabolism; NM, nucleotide metabolism; RNA S, RNA splicing; RNA S-P, RNA splicing, processing; RNA B, RNA binding; RNA M, RNA metabolism; DNA REP, DNA replication; DNA RR, DNA repair; TRL, translation; PRO, proteolysis; ST, signal transduction; T, transport; PT, protein transport; TR, transcription regulator; ANG, angiogenesis; A, adhesion; MIG, migration; I, invasion; AAP, anti-apoptosis; AXO, axonogenesis; and MS, mucus secretion.

were related to transcription, translation, DNA replication and repair, metabolism, protein folding, proteolysis, cytoskeleton filaments reorganization, cell cycle control, cell growth, development, adhesion and migration, immune response, NRF2-mediated oxidative stress responses, and signal transduction (Fig. 1B). The upregulated proteins (>2.5-fold) in more than 9 patients detected by QSTAR Elite LC-MS/MS and IPA in lung adenocarcinomas compared with the adjacent normal tissue are presented in Table 1. We selected tumorigenesis-associated proteins based on the results of ProteinPilot analyses and IPA. Among the identified upregulated extracellular space and cytoplasmic proteins, those most frequently and highly overexpressed proteins in lung adenocarcinoma samples compared with adjacent normal tissue were selected as candidate biomarkers. They included anterior gradient homolog 2 (*Xenopus laevis*) (AGR2) (9.9-fold), ribosome binding protein 1 homolog 180kDa (dog) (RRBP1) (4.9-fold), coatomer protein complex, subunit alpha (COPA) (4.3-fold), thioredoxin domain containing 5 (endoplasmic reticulum) (TXNDC5) (4.1-fold), cytoskeleton-associated protein 4 (CKAP4) (3.6-fold), acidic (leucine-rich) nuclear phosphoprotein 32 family, member A (ANP32A) (3.5 fold), and non-POU domain containing, octamer-binding (NONO) (3.3-fold) (Table 1). The most highly and frequently overexpressed candidate protein, AGR2, was chosen as the most reliable potential biomarker, and its expression was further evaluated in a large number of patients by immunohistochemistry.

***Immunohistochemical staining of AGR2 in lung adenocarcinoma***

To examine the expression of AGR2 protein of lung adenocarcinoma, immunohistochemical staining was performed with a monoclonal antibody specific for AGR2, which did not react with

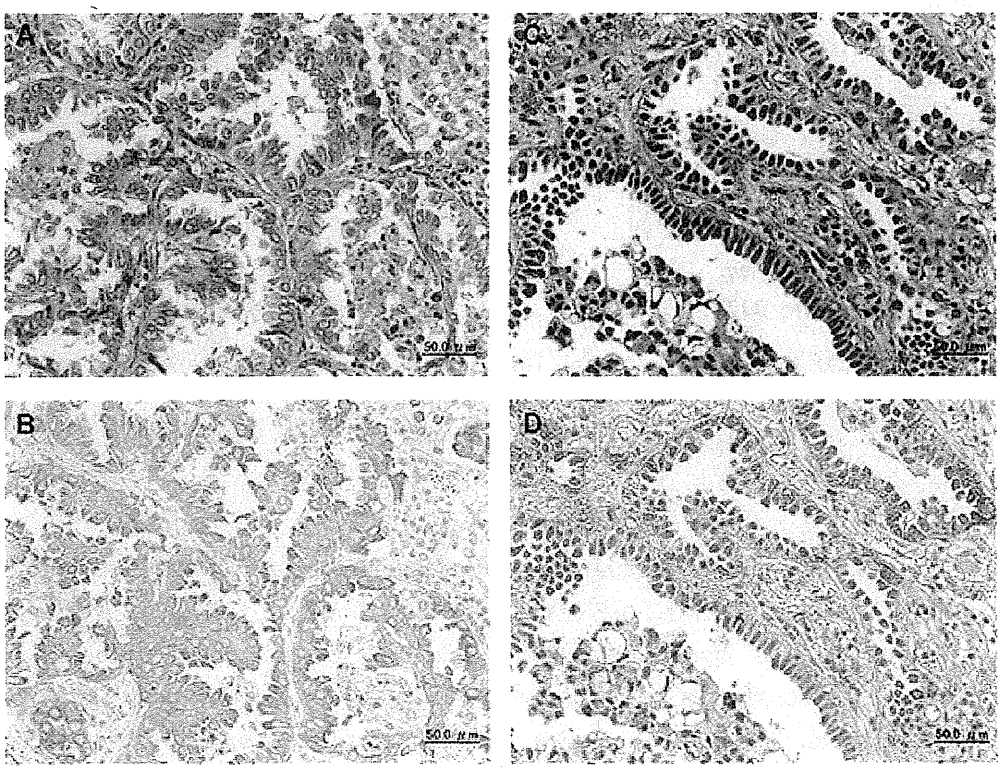


**Figure 2.** Immunohistochemical detection of AGR2 (B and D) and HE stain (A and C) in human lung adenocarcinoma. B, Strong positive staining of AGR2. D, Weak to moderately stained AGR2. AGR2, anterior gradient homolog 2.

AGR3 in samples from 268 patients who underwent surgical resection. Representative staining for AGR2 is shown in Figure 2. In the normal lung tissue, immunohistochemical staining for AGR2 displayed a weak granular cytoplasmic appearance in the bronchial epithelial cells, type 2 alveolar epithelial cells, and secretory epithelial cells of the bronchial gland. By contrast, strongly positive granular cytoplasmic staining for AGR2 was observed in the primary lung adenocarcinoma polarized toward the surface of the papillae, with a prevalent papillary pattern and the less granular pattern, and lacking specific polarization with a prevalent glandular pattern. Staining showed a heterogeneous pattern and great variation from tumor to tumor in the proportion of cancer cells, ranging from no staining to strongly positive staining. AGR2 was mainly positive in the cytoplasm of cancer cells. From 268 cases examined, AGR2 was strongly positive in 196 cases (73.1%; score +2), weakly to moderately positive in 56 cases (20.9%; +1), and negative in 16 cases (6.0%; 0).

***Correlation between AGR2 expression and clinical outcomes of patients with lung adenocarcinoma***

**Table 2. Association between AGR2 staining grade and clinicopathological parameters**

| | No. of patients | | | | p value |
|---|---|---|---|---|---|
| | Total | Negative | Positive (1+) | Positive (2+) | |
| Age | | | | | |
| <65 | 114 | 7 | 20 | 87 | 0.509 |
| ≧65 | 154 | 9 | 36 | 109 | |
| Gender | | | | | |
| male | 155 | 12 | 30 | 113 | 0.308 |
| female | 113 | 4 | 26 | 83 | |
| Smoking | | | | | |
| nonsmoker | 101 | 5 | 21 | 75 | 0.856 |
| smoker | 167 | 11 | 35 | 121 | |
| Differentiation | | | | | |
| well | 77 | 7 | 23 | 47 | 0.085* |
| moderate | 117 | 6 | 20 | 91 | |
| poor | 74 | 3 | 13 | 58 | |
| pT factor | | | | | |
| T1 | 144 | 9 | 30 | 105 | 0.979 |
| T2-4 | 124 | 7 | 26 | 91 | |
| pN factor | | | | | |
| N0 | 186 | 11 | 38 | 137 | 0.972 |
| N1-3 | 82 | 5 | 18 | 59 | |
| pStage | | | | | |
| Ⅰ | 157 | 10 | 31 | 116 | 0.989* |
| Ⅱ | 26 | 1 | 7 | 18 | |
| Ⅲ | 68 | 4 | 14 | 50 | |
| Ⅳ | 17 | 1 | 4 | 12 | |

Fisher's exact test; *Chi square test; pT factor, pathological T factor; pN factor, pathological N factor; pStage, pathological stage; and AGR2, anterior gradient homolog 2.

We evaluated the correlation between AGR2 expression and clinicopathological outcomes using a chi squared test. As shown in Table 2, intensities of AGR2 expression (score 0, +1, +2) were not significantly associated with age (<65, ≧65; p=0.509), gender (male, female; p=0.308), smoking history (nonsmoker, smoker; p=0.856), histological differentiation (well, moderate, poor differentiation; p=0.085), pT factor (pT1, pT2-4; p=0.979), pN factor (pN0, pN1-3; p=0.972), or disease stage (Ⅰ, Ⅱ, Ⅲ, Ⅳ; p=0.989). To evaluate associations between cancer prognosis and intensity of AGR2 expression (score 0, +1 versus +2), apart from the established prognostic factors of pT status, pN status, histological differentiation, and disease stage, univariate survival analysis was performed with disease-specific survival curves according to the Kaplan-Meier method and differences in survival were assessed with the log-rank test (Fig. 3). From these results, negative AGR2 expression was found to be significantly associated with poor prognosis compared with the strongly positive expression (p=0.007). The decrease in intensity of AGR2 expression was associated with the poorer survival; however, statistical significance was not reached between negative and weak to moderately positive AGR2 expression, and between weak to moderately positive and strongly positive AGR2 expression. In Cox multivariate analysis, AGR2 expression changes were not significant (data not shown).

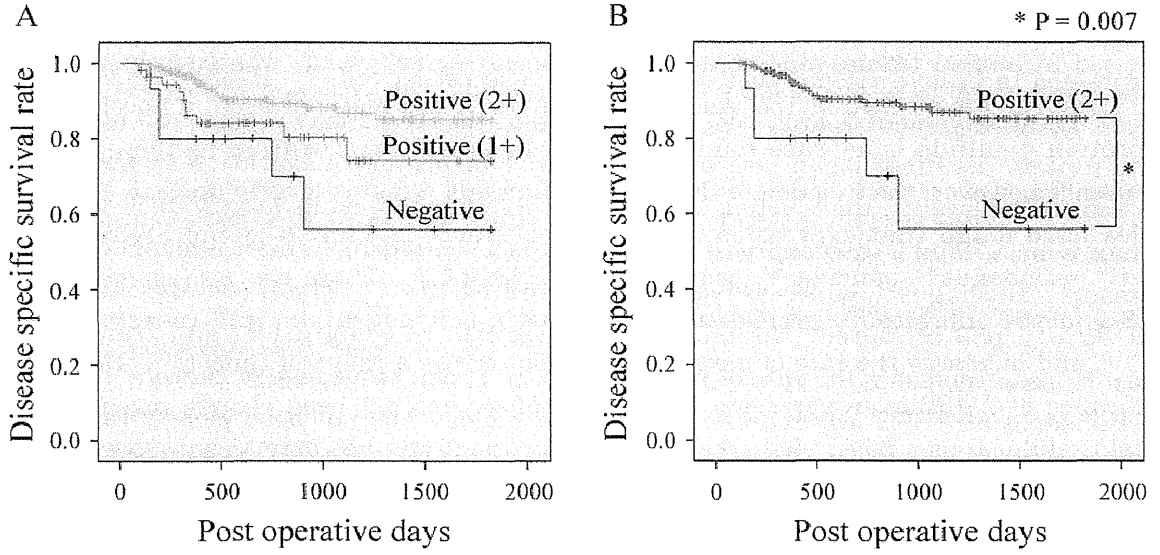


**Figure 3.** Kaplan-Meier curves for disease-specific survival. A, Survival curves for AGR2 positive (2+), positive (1+), and negative expression in human lung adenocarcinoma. B, Survival curves for AGR2 positive (2+) and negative expression. AGR2, anterior gradient homolog 2.

## Discussion

In proteomic analyses of clinical oncology, the main purpose is the selection and validation of proteins that are potential biomarkers, which are identified and quantified by proteomic techniques, including LC-MS/MS coupled with iTRAQ technology. The ultimate purpose is the clarification of pathological functions of proteins related to carcinogenesis, and the development of diagnostic procedures and new therapeutic strategies. Many proteomics studies have been performed to discover new markers for lung cancer using human materials such as cancer tissue, plasma, and pleural effusion of lung cancer patients; however, no new reliable biomarker has been applied in the clinical setting. Liquid chromatography-tandem mass spectrometry makes it

possible to analyze and identify a great number of proteins and peptides concurrently, and the iTRAQ technology allows multiplexed relative quantitative proteome analysis under the same experimental conditions and, with a combination with LC-MS/MS techniques, has increased the analytical accuracy of results[4-6,8-10].

Here, we were able to identify several new proteins that were strongly and frequently overexpressed in human lung adenocarcinoma compared with the adjacent normal lung tissue, which were evaluated as potential biomarkers. To the best of our knowledge, this is the first experimental evidence of significant overexpression of AGR2, RRBP1, COPA, TXNDC5, CKAP4, ANP32A, and NONO based on the proteome analysis. Furthermore, significantly high overexpression of AGR2 detected by both proteome and immunohistochemical techniques indicated that this protein is a potential biomarker of human adenocarcinoma. A large number of human lung adenocarcinoma samples (252/268) proved to be AGR2 positive.

AGR2, also known as hAG-2[11] and Gob-4[12], is the human ortholog of the secreted *X. laevis* Anterior Gradient protein (XAG-2). In the *X. laevis* embryo, XAG-2 protein is highly expressed in the mucus-secreting cement gland and induces cement gland differentiation, ectodermal patterning, and expression of neural marker genes in a fibroblast growth factor-dependent manner[13-16]. The function of XAG-2 in adult *X. laevis* is largely unknown. The AGR2 protein consists of 175 amino acids with a molecular weight of approximately 20000 Da, and is widely expressed in human tissues that contain mucus-secreting cells[11]. It was suggested, based on Basic Local Alignment Search Tool Analysis[17], that the AGR2 may represent a novel member of the protein disulfide isomerase family involved in protein maturation in the endoplasmic reticulum[18]; however, the function of the AGR2 in humans remains largely unclear. Subsequent studies have found that expression of AGR2 is elevated in human adenocarcinoma of the breast[14], esophagus[19], pancreas[20], prostate[21], and NSCLC[22]. There are also suggestions that AGR2 is a p53 inhibitor[19], promotes tumor growth, cell migration, and transformation *in vitro*[20,23], and increases the rate of metastasis *in vivo*, across a range of cancers[24]. However, the significance of AGR2 overexpression in cancer biology has not been clearly revealed and its clinical usefulness as a novel biomarker and therapeutic target has only recently been proposed. With regards to NSCLC, it has been reported that the AGR2 is strongly upregulated in lung adenocarcinoma cell lines, indicating that it is a novel candidate oncogene in lung cancer[25]. It has been also observed that AGR2 is commonly overexpressed in NSCLC tissue and that its expression is associated with the negative residual status of patients; however, its prognostic value could not be demonstrated[22].

In the present study, negative AGR2 expression was associated with poor prognosis of lung cancer. There are three reports on the association between AGR2 expression and prognosis of breast cancer[26-28]. In the study of Fritzsche et al, expression of AGR2 in breast cancer cells was associated with significantly longer survival of 155 breast carcinoma patients treated with various adjuvant therapies[27]. In another study, in 351 breast cancer patients treated by adjuvant hormonal therapy, upregulation of AGR2 was associated with a poor prognosis in patients with ERα-positive breast cancers after treatment with anti-estrogen therapy[28]. Barraclough et al have shown that the presence of AGR2 in the primary tumor is a possible prognostic indicator of poor outcome in 315 patients suffering from operable (stage Ⅰ and Ⅱ) breast cancer[26]. Furthermore, in prostate cancer, it was reported that elevated AGR2 was

significantly associated with poor patient survival[29].

In conclusion, in this study, AGR2 was evaluated as a potential biomarker of lung adenocarcinoma based on combined proteomic and immunohistochemical analyses of a large number of patients. Its negative tumor tissue expression was associated with poor disease-specific survival. Further studies are required to clarify the biological significance of AGR2 overexpression in adenocarcinoma and, ultimately, to evaluate its usefulness as a novel diagnostic or prognostic biomarker and therapeutic target in clinical practice.

## Acknowledgements

We thank Azusa Inagaki and Kaori Touma for their technical assistance, and Yukiko Iura for her help during the preparation of this manuscript. This work was supported by a Grant-in-Aid for Scientific Research from the Ministry of Education, Culture, Sports, Science and Technology of Japan.

## References

1. Vielh P, Spano JP, Grenier J, Le Chevalier T, Soria JC. Molecular prognostic factors in resectable non-small cell lung cancer. Crit Rev Oncol Hematol 2005;53:193-197.
2. Tarro G, Perna A, Esposito C. Early diagnosis of lung cancer by detection of tumor liberated protein. J Cell Physiol 2005;203:1-5.
3. McCarthy NJ, Swain SM. Tumor markers: should we or shouldn't we? Cancer J 2001;7:175-177.
4. Ross PL, Huang YN, Marchese JN, Williamson B, Parker K, Hattan S, et al. Multiplexed protein quantitation in Saccharomyces cerevisiae using amine-reactive isobaric tagging reagents. Mol Cell Proteomics 2004;3:1154-1169.
5. Kakehashi A, Ishii N, Shibata T, Wei M, Okazaki E, Tachibana T, et al. Mitochondrial prohibitins and septin 9 are implicated in the onset of rat hepatocarcinogenesis. Toxicol Sci 2011;119:61-72.
6. Kakehashi A, Kato A, Inoue M, Ishii N, Okazaki E, Wei M, et al. Cytokeratin 8/18 as a new marker of mouse liver preneoplastic lesions. Toxicol Appl Pharmacol 2010;242:47-55.
7. Song X, Bandow J, Sherman J, Baker JD, Brown PW, McDowell MT, et al. iTRAQ experimental design for plasma biomarker discovery. J Proteome Res 2008;7:2952-2958.
8. DeSouza L, Diehl G, Rodrigues MJ, Guo J, Romaschin AD, Colgan TJ, et al. Search for cancer markers from endometrial tissues using differentially labeled tags iTRAQ and cICAT with multidimensional liquid chromatography and tandem mass spectrometry. J Proteome Res 2005;4:377-386.
9. Garbis SD, Tyritzis SI, Roumeliotis T, Zerefos P, Giannopoulou EG, Vlahou A, et al. Search for potential markers for prostate cancer diagnosis, prognosis and treatment in clinical tissue specimens using amine-specific isobaric tagging (iTRAQ) with two-dimensional liquid chromatography and tandem mass spectrometry. J Proteome Res 2008;7:3146-3158.
10. Zieske LR. A perspective on the use of iTRAQ reagent technology for protein complex and profiling studies. J Exp Bot 2006;57:1501-1508.
11. Thompson DA, Weigel RJ. hAG-2, the human homologue of the Xenopus laevis cement gland gene XAG-2, is coexpressed with estrogen receptor in breast cancer cell lines. Biochem Biophys Res Commun 1998;251:111-116.
12. Komiya T, Tanigawa Y, Hirohashi S. Cloning of the gene gob-4, which is expressed in intestinal goblet cells in mice. Biochim Biophys Acta 1999;1444:434-438.
13. Aberger F, Weidinger G, Grunz H, Richter K. Anterior specification of embryonic ectoderm: the role of the Xenopus cement gland-specific gene XAG-2. Mech Dev 1998;72:115-130.
14. Fletcher GC, Patel S, Tyson K, Adam PJ, Schenker M, Loader JA, et al. hAG-2 and hAG-3, human homologues of genes involved in differentiation, are associated with oestrogen receptor-positive breast tumours and interact with metastasis gene C4.4a and dystroglycan. Br J Cancer 2003;88:579-585.
15. Sive H, Bradley L. A sticky problem: the Xenopus cement gland as a paradigm for anteroposterior patterning. Dev Dyn 1996;205:265-280.
16. Sive HL, Hattori K, Weintraub H. Progressive determination during formation of the anteroposterior axis in Xenopus laevis. Cell 1989;58:171-180.

17. Altschul SF, Madden TL, Schäffer AA, Zhang J, Zhang Z, Miller W, et al. Gapped BLAST and PSI-BLAST: a new generation of protein database search programs. Nucleic Acids Res 1997;25:3389-3402.
18. Persson S, Rosenquist M, Knoblach B, Khosravi-Far R, Sommarin M, Michalak M. Diversity of the protein disulfide isomerase family: identification of breast tumor induced Hag2 and Hag3 as novel members of the protein family. Mol Phylogenet Evol 2005;36:734-740.
19. Pohler E, Craig AL, Cotton J, Lawrie L, Dillon JF, Ross P, et al. The Barrett's antigen anterior gradient-2 silences the p53 transcriptional response to DNA damage. Mol Cell Proteomics 2004;3:534-547.
20. Ramachandran V, Arumugam T, Wang H, Logsdon CD. Anterior gradient 2 is expressed and secreted during the development of pancreatic cancer and promotes cancer cell survival. Cancer Res 2008;68:7811-7818.
21. Zhang JS, Gong A, Cheville JC, Smith DI, Young CY. AGR2, an androgen-inducible secretory protein overexpressed in prostate cancer. Genes Chromosomes Cancer 2005;43:249-259.
22. Fritzsche FR, Dahl E, Dankof A, Burkhardt M, Pahl S, Petersen I, et al. Expression of AGR2 in non small cell lung cancer. Histol Histopathol 2007;22:703-708.
23. Wang Z, Hao Y, Lowe AW. The adenocarcinoma-associated antigen, AGR2, promotes tumor growth, cell migration, and cellular transformation. Cancer Res 2008;68:492-497.
24. Liu D, Rudland PS, Sibson DR, Platt-Higgins A, Barraclough R. Human homologue of cement gland protein, a novel metastasis inducer associated with breast carcinomas. Cancer Res 2005;65:3796-3805.
25. Zhu H, Lam DC, Han KC, Tin VP, Suen WS, Wang E, et al. High resolution analysis of genomic aberrations by metaphase and array comparative genomic hybridization identifies candidate tumour genes in lung cancer cell lines. Cancer Lett 2007;245:303-314.
26. Barraclough DL, Platt-Higgins A, de Silva Rudland S, Barraclough R, Winstanley J, West CR, et al. The metastasis-associated anterior gradient 2 protein is correlated with poor survival of breast cancer patients. Am J Pathol 2009;175:1848-1857.
27. Fritzsche FR, Dahl E, Pahl S, Burkhardt M, Luo J, Mayordomo E, et al. Prognostic relevance of AGR2 expression in breast cancer. Clin Cancer Res 2006;12:1728-1734.
28. Innes HE, Liu D, Barraclough R, Davies MP, O'Neill PA, Platt-Higgins A, et al. Significance of the metastasis-inducing protein AGR2 for outcome in hormonally treated breast cancer patients. Br J Cancer 2006;94:1057-1065.
29. Zhang Y, Forootan SS, Liu D, Barraclough R, Foster CS, Rudland PS, et al. Increased expression of anterior gradient-2 is significantly associated with poor survival of prostate cancer patients. Prostate Cancer Prostatic Dis 2007;10:293-300.

# MUC5AC protects pancreatic cancer cells from TRAIL-induced death pathways

HIROTAKA HOSHI[1,3], TETSUJI SAWADA[2], MOTOYUKI UCHIDA[1], HIROKO IIJIMA[1], KENJIRO KIMURA[2], KOSEI HIRAKAWA[2] and HIDEKI WANIBUCHI[3]

[1]Biomedical Research Laboratories, Kureha Corporation, Shinjuku-ku, Tokyo 169-8503; Departments of [2]Surgical Oncology and [3]Pathology, Osaka City University Graduate School of Medicine, Abeno-ku, Osaka 545-8585, Japan

Received September 3, 2012; Accepted November 12, 2012

DOI: 10.3892/ijo.2013.1760

**Abstract.** We have previously reported that a specific siRNA transfected MUC5AC could knockdown MUC5AC expression and suppress *in vivo* tumor growth and metastasis, although it had no effects on *in vitro* cell growth, cell survival, proliferation and morphology. In the present study, we investigated which host immune cells induced these effects and how the effects were induced using immunocyte-depleted animal models. The tumor growth of SW1990/si-MUC5AC cells, which show no tumor growth when implanted subcutaneously into a nude mouse, was recovered when neutrophils were removed by anti-Gr-1 mAb administration. This result suggests that MUC5AC may suppress the antitumor effects of neutrophils by allowing tumor cells to escape the host immune system. Subsequently, we investigated the effects of MUC5AC on apoptosis induction mediated by TNF-related apoptosis-inducing ligand (TRAIL), one of the antitumor mechanisms of neutrophils. SW1990/si-MUC5AC cells showed significantly increased active caspase 3 expression after the addition of TRAIL. On the other hand, SW1990/si-mock cells showed no such changes. Our results indicate that MUC5AC inhibits TRAIL-induced apoptosis in human pancreatic cancer and may serve as an important indicator in diagnosis and prognosis.

## Introduction

Pancreatic cancer is the 8th and 9th leading cause of cancer-related deaths worldwide in men and women. More than 50% of patients are diagnosed with advanced disease and have metastatic disease at presentation, 10 to 15% will be resectable, and the remainder will be locally advanced unresectable disease as well as an incidence of unrecognized metastases. The majority of patients have a median survival with treatment of less than 6 months. Even for those seemingly fortunate enough to have early-stage local and resectable disease, the 5-year survival is only 20% after resection (1). Therefore, pancreatic cancer is a refractory cancer having poor prognosis.

MUC5AC is a member of the secreted mucin family and is expressed as secretory mucin from goblet cells of the stomach, airways and cervical secretion. These cover the epithelium and provide a lubricating barrier that protects the mucosal surface. On the other hand, it is overexpressed as a membrane-bound type in the ductal region of human pancreatic cancer, while remaining undetectable in the normal pancreas. However, there have been few reports on the function of MUC5AC in pancreatic cancer (2-4).

The dominant view of polymorphonuclear neutrophils (PMNs) is that they are of the most abundant and short-lived in total circulating blood leukocytes and their cytoplasm has highly developed cytomatrices and granules containing microbicidal proteins and digestive enzymes. They provide the first-line of defense against various infections, are potent effectors of inflammation, and release chemotactic factors that lead to the recruitment of non-specific and specific immune effectors (5). Studies on the immunological mechanisms have focused mainly on the function of lymphocytes and monocytes/macrophages as important mediators of the host response. However, PMNs are increasingly recognized as an important effector cell population for the rejection of malignant tumors *in vivo*, including Fas ligand-mediated apoptosis, antibody-dependent cellular cytotoxicity (ADCC), direct cell killing by $H_2O_2$ and superoxide and calprotectin (6,7).

The antitumor molecule TNF-related apoptosis-inducing ligand (TRAIL) has been reported previously (8,9) and is part of the TNF superfamily member, is expressed in a broad range of cells including activated T cells, B cells, natural killer cells, dendritic cells, monocytes and activated neutrophils, and exerts great antitumor activity. It is known that TRAIL is highly expressed on neutrophils selectively inducing apoptosis. TRAIL exerts its activity by interacting with a complex system of 2 death receptors (DRs) (DR4/TRAIL-R1 and DR5/TRAIL-R2) and 3 decoy receptors (DcRs) [DcR1/TRAIL-R3, DcR2/TRAIL-R4

*Correspondence to:* Dr Tetsuji Sawada, Department of Surgical Oncology, Osaka City University Graduate School of Medicine, 1-4-3 Asahi-machi, Abeno-ku, Osaka 545-8585, Japan
E-mail: t_sawada@osaka-ekisaikai.jp

*Key words:* MUC5AC, mucin, pancreatic cancer, short interfering RNA, TNF-related apoptosis-inducing ligand, apoptosis

and osteoprotegerin (OPG)]. Although these receptors are characterized by high sequence homology in their extracellular domains, only DR4/TRAIL-R1 and DR5/TRAIL-R2 contain a functionally active death domain that allows an apoptotic response by TRAIL stimulation (10,11). Some correlations between TRAIL sensitivity and receptor expression have been reported in various tumor cells. TRAIL only acts on cancer cells, it does not act on normal cells. Although there is a theory that this reason is due to a difference in expression levels of death receptors and decoy receptors on these cells, the detailed mechanisms are not known. In our previous study, when MUC5AC-expressing pancreatic cancer cells were knocked down for MUC5AC by specific siRNA, cell survival, proliferation, and morphology *in vitro* were the same as control cells. However, their tumor growth in *in vivo* xenograft studies was significantly lower than that of control cells and most infiltrated leukocytes, particularly neutrophils and B cells, were observed to be accumulated into its tumor challenged site. Moreover, a greater number of antibodies against cancer cells were found in the blood of SW1990/si-MUC5AC cell-challenged mice than that of SW1990/si-mock cell-challenged mice. As a result, it appeared that the tumorigenicity and growth of MUC5AC knockdown cells were significantly lower than that of control cells (12).

In the present study, we assessed the mechanisms of MUC5AC on these immune cells using the neutrophil depletion model by anti-Gr-1 mAb and SCID mice in which B and T cells were depleted. Furthermore, we focused on the anti-tumor effects of neutrophils and hypothesized that MUC5AC was able to inhibit apoptosis via TRAIL signaling pathways. To investigate the function of MUC5AC in pancreatic cancer, we evaluated whether or not MUC5AC knockdown would increase TRAIL responsiveness such as the expression of TRAIL receptor and the effects on apoptosis signaling pathways in pancreatic cancer cells.

## Materials and methods

*Reagents*. Recombinant human TRAIL was purchased from PeproTech GmbH (Paris, France). The tetrapeptide caspase inhibitor z-VAD-fmk was obtained from R&D Systems (Minneapolis, MN). The rat anti-mouse Gr-1 monoclonal antibody used for deplete murine neutrophils was from BD Pharmingen Inc. (San Diego, CA). GeneJuice used for siRNA transfection was purchased from Merck (Darmstadt, Germany).

*Animals*. Specific-pathogen-free female BALB/c-nu/nu mice (nude mice) and C.B17-scid/scid mice (SCID mice) purchased from Charles River Japan Inc. (Kanagawa, Japan) were acclimatized and then used in experiments at the age of six weeks. The experimental design was approved by the Ethics Committee on Animal Experiments of the Biomedical Research Laboratories of Kureha Corp., and mice were treated in accordance with the guidelines of the committee. All animals were allowed free access to sterilized CE-2 food (Oriental Yeast, Tokyo, Japan) and sterilized tap water. Mice were bred at 25±2˚C, a humidity of 55±7%, laminar flow, and under a 12 h light/12 h dark cycle at 150-300 lux. To maintain a uniform environment, noise was carefully avoided and only experimental staff and keepers were allowed into the animal room.

*Cell culture conditions*. SW1990 was cultured in Dulbecco's modified Eagle's medium (DMEM; Invitrogen Corporation, San Diego, CA) supplemented with 10% fetal bovine serum (FBS; Biowest, Nuaill, France), 50 IU/ml penicillin and 50 $\mu$g/ml streptomycin. Cells were grown at 37˚C with 5% $CO_2$ in a humidified atmosphere and passaged before they reached confluency using 0.25% (w/v) trypsin solution containing 0.04% (w/v) EDTA.

*Construction of siRNA-MUC5AC and establishing the stable expression cell line*. The MUC5AC siRNA target sequence 5'-TTTGAGAGACGAAGGATAC-3' was cloned to generate a stable siRNA expressing construct into the p*Silencer* 3.1-H1 neo vector (Ambion Inc., Austin, TX) as described previously (12). SW1990 cells were transfected with p*Silencer*/si-MUC5AC as a target or p*Silencer*/si-mock as a control using GeneJuice according to the manufacturer's instructions. SW1990 cells were selected by culturing in the presence of geneticin at 600 $\mu$g/ml. The efficiency of MUC5AC-knockdown was tested through RT-PCR and FACS analysis (data not shown).

*Preparation of neutrophil-depleted mice*. Neutrophils were depleted from nude mice using anti-Gr-1 mAb. Anti-Gr-1 mAb was treated at single doses of 100 $\mu$g/mice via i.p. injection on days -1, 4, 9, 14, 19, 24, 29, 34 and 39. The depletion of neutrophils was determined before tumor cell implantation by a flow cytometer (13).

*Tumorigenicity assay in xenograft models*. Cells were implanted subcutaneously (s.c.) at $1x10^7$/mice on the flank of nude mice or SCID mice. Tumor volumes were measured at least once a week. For the determination of tumor volume, two bisecting diameters of each tumor were measured by slide calipers and tumor volumes were calculated using the following formula: tumor volume = length x $(\text{width})^2$ x 0.5236. Eight mice were used for each cell line. Tumor growth curves were plotted as the mean volume ± standard error (SE).

*Apoptosis assays*. SW1990/si-MUC5AC cells and SW1990/si-mock cells ($2x10^3$ cells/100 $\mu$l) were cultured in 96-well plates in medium containing recombinant human TRAIL at fixed concentrations. Cell proliferation was evaluated by the MTT assay as previously described (12). The pan-caspase inhibitor z-VAD-fmk was dosed at 10 $\mu$M before 1 h of TRAIL treatment.

*Human apoptosis array*. The expression profile of apoptosis-related proteins was detected and analyzed using a Proteome Profiler™ (R&D Systems Inc.) according to the manufacturer's instructions. Briefly, protein lysates (500 $\mu$g) from SW1990/si-MUC5AC cells and SW1990/si-mock cells were loaded onto an array membrane blocked with blocking reagent. The membrane was incubated overnight at 4˚C, washed thrice with TBST, and then incubated with a detection antibody cocktail for 1 h. After three TBST washes,

spots were visualized by a chemiluminescence assay and the average density of duplicate spots was recorded.

*Production of IL-8.* SW1990/si-MUC5AC cells and SW1990/si-mock cells ($10^4$ cells/100 $\mu$l) were cultured in 96-well plates for 2 or 4 days. Culture supernatants were collected and measured using a human IL-8 ELISA kit (RayBiotech Inc., Norcross, GA), as directed by the manufacturer.

*Statistical analysis.* All data are expressed as the means ± SE. Statistical significance was determined by the Student's t-test. P-values <0.05 were considered significant.

## Results

*Effects of MUC5AC on immunocytes.* Previous studies have demonstrated that the tumor growth of MUC5AC-knockdown cells is markedly suppressed when they are subcutaneously implanted into a nude mouse. Furthermore, neutrophils and B cells accumulated in the tumor (12). Thus, in the present study, we investigated the effects of neutrophils and B cells on the tumor growth of MUC5AC-expressing cells and the immune evasion mechanism through MUC5AC.

First, to examine the involvement of B cells on the tumor growth of MUC5AC-expressing cells, we investigated the tumor growth of MUC5AC-expressing and MUC5AC-knockdown cells in SCID mice. SW1990/si-MUC5AC or SW1990/si-mock cells were implanted subcutaneously into SCID mice at $1x10^7$ cells/mice and then tumor volume was assessed. If B cells act directly on the antitumor effects of MUC5AC-knockdown-challenged mice, MUC5AC-knockdown cells should grow comparably to MUC5AC-expressing cells. However, the tumor volume of SW1990/si-mock cells increased over time, while that of SW1990/si-MUC5AC cells barely increased and little tumor growth was observed (Fig. 1A).

Subsequently, to examine the involvement of MUC5AC on the antitumor effects of neutrophils, 100 $\mu$g of anti-Gr-1 antibody was administered once every five days to a nude mouse to deplete neutrophils. Neutrophil depletion was confirmed by FACS before tumor implantation (data not shown). SW1990/si-MUC5AC or SW1990/si-mock cells were implanted subcutaneously at $1x10^7$ cells/nude mouse, and then tumor volume was assessed. The tumor growth of SW1990/si-MUC5AC cells was barely observed in the presence of neutrophils (Fig. 1B). However, tumor growth recovered to the same level as SW1990/si-mock cells when neutrophils were depleted with an anti-Gr-1 antibody (Fig. 1C).

*MUC5AC suppresses IL-8 production of tumor cells.* IL-8 produced by peripheral tissue cells and activated neutrophils is involved in the migration of neutrophils into the tissue (8). Hence, the amounts of *in vitro* IL-8 production were determined in SW1990/si-MUC5AC and SW1990/si-mock cells. IL-8 concentrations in the supernatants of SW1990/si-MUC5AC and SW1990/si-mock cells were 1,529 and 179 ng/ml on day 2 and 4,100 and 1,094 ng/ml on day 4, respectively. Suppressed MUC5AC expression significantly increased IL-8 production (Fig. 2).

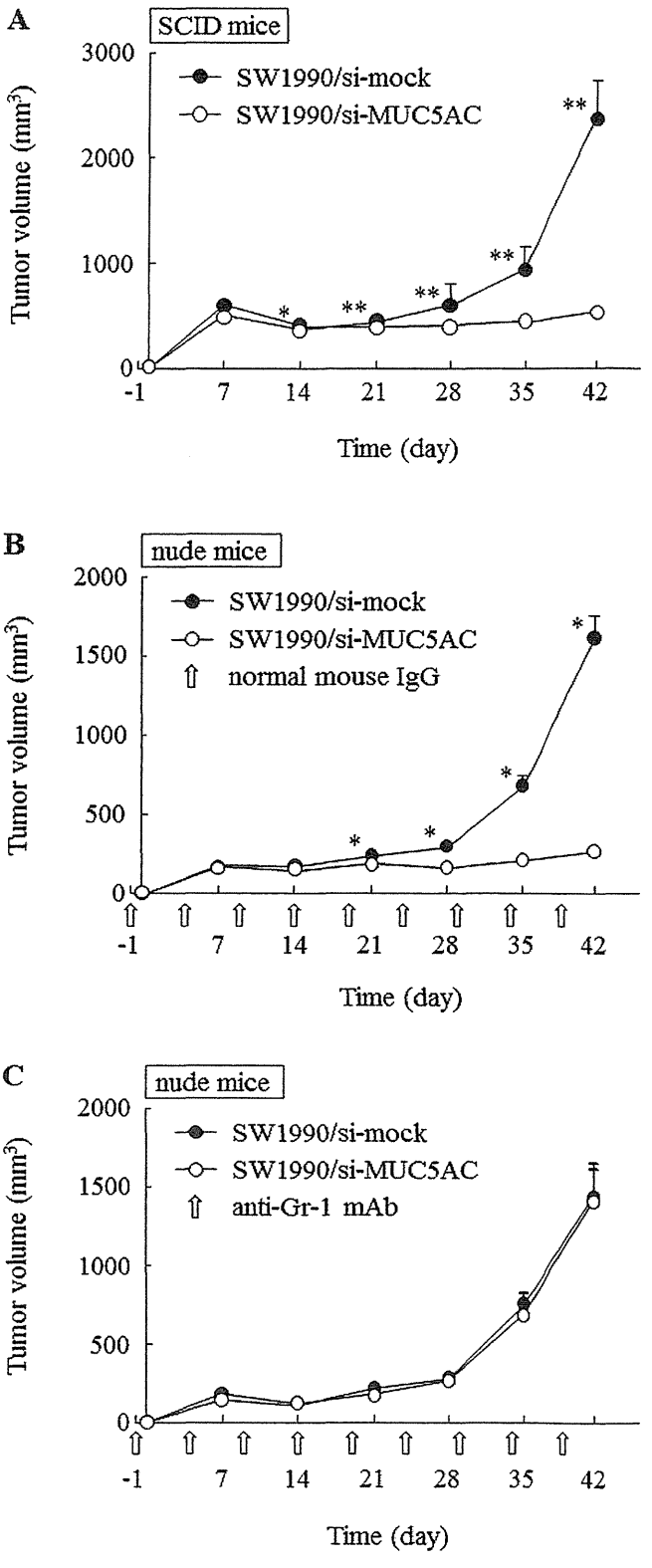


Figure 1. MUC5AC suppresses the antitumor processes of neutrophils. (A) Tumor growth curves of SW1990/si-mock cells (filled circles) and SW1990/si-MUC5AC cells (open circle). Cells were s.c. implanted with $1x10^7$ cells into SCID mice on day 0. (B) Tumor growth curves of SW1990/si-mock cells (filled circles) and SW1990/si-MUC5AC cells (open circle) in normal mouse IgG-treated nude mice. (C) Tumor growth curves of SW1990/si-mock cells (filled circles) and SW1990/si-MUC5AC cells (open circle) in anti-Gr-1 mAb-treated mice. Cells were s.c. implanted with $1x10^7$ cells into nude mice on day 0. Mice were monitored for tumor formation until 42 days and tumor sizes were measured on indicated days. These experiments were performed at least twice and representative data are shown. Points, tumor volume of 8 mice for each group; bars, SE. *P<0.05 and **P<0.001.

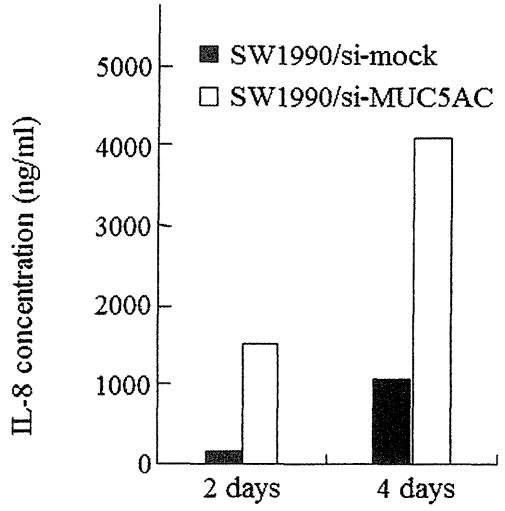


Figure 2. Knockdown of MUC5AC stimulates IL-8 production in pancreatic cancer cells. Cells ($10^4$ cells/100 $\mu$l) were cultured in 96-well plates for 2 or 4 days. Culture supernatants were collected and measured using a human IL-8 ELISA kit. Results were averaged from 3 separate experiments. One representative of at least three similar experiments is shown.

*MUC5AC inhibits TRAIL-induced apoptosis.* It is known that activated neutrophils produced TRAIL, which in turn, induced apoptosis of cancer cells via its death receptors. Therefore, we evaluated cell viability after TRAIL treatment by the MTT assay. The correlation between the dose of TRAIL and cell growth inhibition is illustrated in Fig. 3A. Our previous reports show that no difference in cell proliferation was observed between SW1990/si-MUC5AC cells and SW1990/si-mock cells under normal conditions *in vitro* (12). After 12 h of TRAIL treatment, cell death was induced in SW1990/si-MUC5AC cells in a dose-dependent manner. In this condition, the $IC_{50}$ value of TRAIL was 5.8 ng/ml. In contrast, treatment of SW1990/si-mock cells at a concentration of TRAIL up to 100 ng/ml resulted in <10% cell death. Concerning cell morphologic changes, SW1990/si-MUC5AC cells were rounded and floating in the medium, while SW1990/si-mock cells still formed a typical epithelioid monolayer at a TRAIL concentration of 100 ng/ml for 4 h (Fig. 3B). Consequently, to examine whether caspases were involved in TRAIL-induced apoptosis in SW1990/si-MUC5AC cells, either the pan-caspase inhibitor z-VAD-fmk (10 $\mu$M) or a vehicle control was added to the culture 1 h before TRAIL treatment (10 ng/ml, 4 h). The results indicated that z-VAD-fmk completely blocked TRAIL-induced apoptosis and caspase activation is a required signal event for TRAIL-induced apoptosis. As shown in Fig. 3C, the percentage of cell viability in SW1990/si-MUC5AC cells by the DMSO vehicle control was 92 and TRAIL treatment was 47% in SW1990/si-MUC5AC cells. In contrast, pretreatment of SW1990/si-MUC5AC cells with z-VAD-fmk followed by TRAIL treatment significantly increased cell viability to 93%.

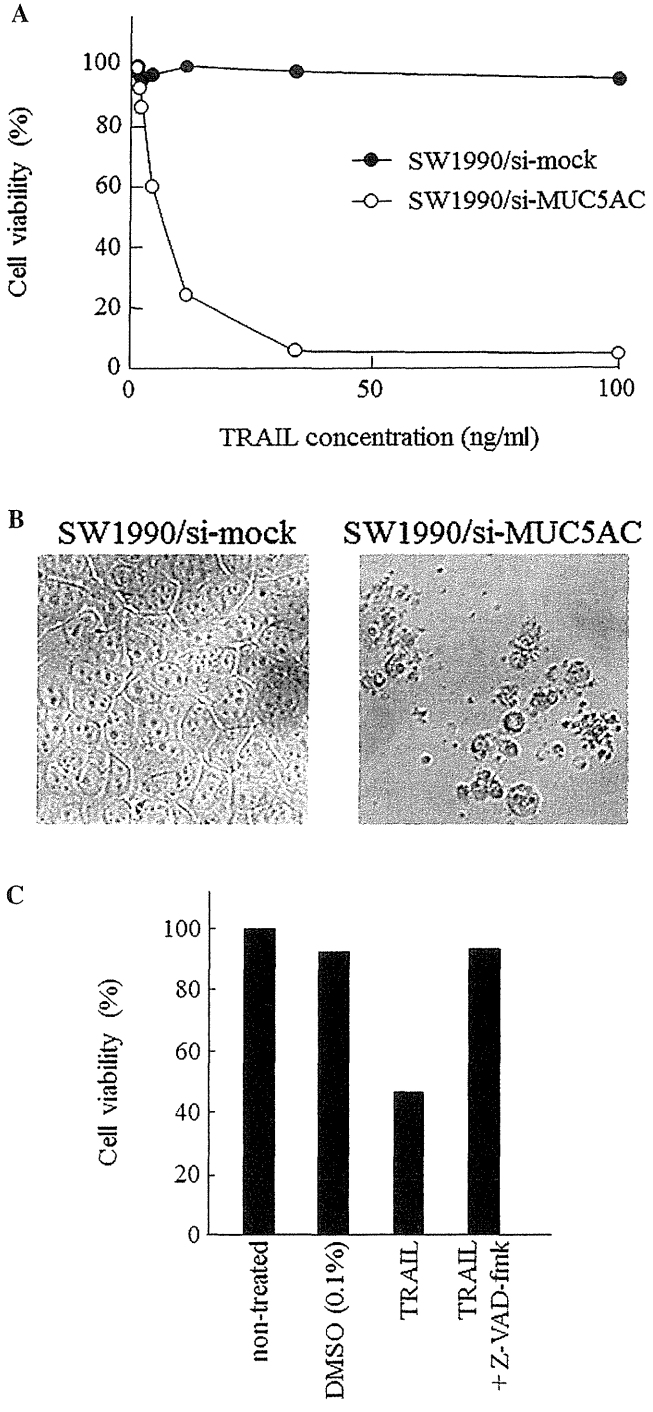


Figure 3. TRAIL induced-apoptosis is stimulated by knockdown of MUC5AC. (A) Cells ($2x10^3$ cells/100 $\mu$l) were cultured in 96-well plates in medium containing recombinant human TRAIL at 0-100 $\mu$g/ml. After 12 h, cell proliferation was evaluated by the MTT assay. (B) Cells were treated with 100 ng/ml of TRAIL for 4 h. Cells were photographed under a phase-contrast microscope. The representative of three independent experiments is shown. (C) Cells ($2x10^3$ cells/100 $\mu$l) were cultured in 96-well plates in medium containing the pan-caspase inhibitor z-VAD-fmk at a dose of 10 $\mu$M for 1 h. Twenty ng/ml of TRAIL was treated for 4 h. Cell numbers were determined by the MTT assay.

*Analysis of the apoptosis suppression mechanism of MUC5AC using an apoptosis array.* As described above, MUC5AC knockdown with siRNA induced apoptosis mediated by TRAIL. Then, to examine differences in the apoptotic signal between SW1990/si-MUC5AC and SW1990/si-mock cells, protein levels relating to apoptosis after the addition of TRAIL to the cells were analyzed using an apoptosis array. Cells were treated with 10 ng/ml of TRAIL for 4 h. The signal intensities in the apoptosis array (Fig. 4A) were digitized and normalized for the positive control value (Fig. 4B). The vehicle control

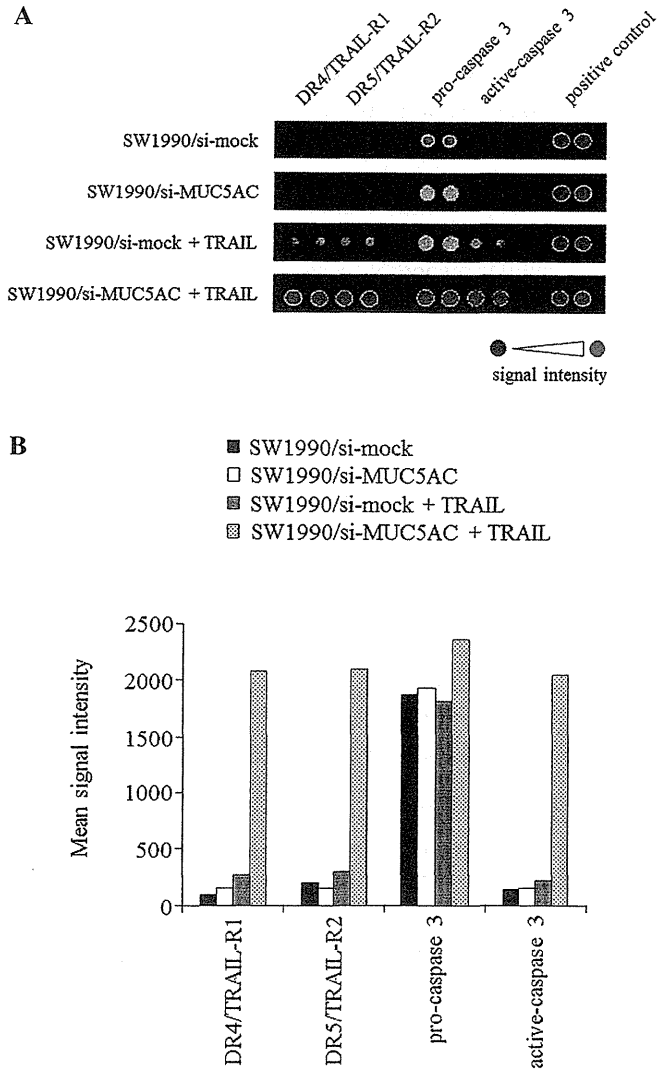


Figure 4. Apoptosis array analysis of pancreatic cancer cells upon knockdown of MUC5AC. (A) Total protein lysates (500 $\mu$g) from SW1990/si-mock cells and SW1990/si-MUC5AC cells were analyzed using Proteome Profiler™. Depicted are representative images of chemiluminescence signals with differences in signal intensities between si-MUC5AC and si-mock cells. One representative of duplicate experiments is shown. (B) Densitometric analysis of apoptosis array blots. Values relative to DR4/TRAIL-R1 expression levels of SW1990/si-mock values set to 100. Means are averaged from 2 spots.

for SW1990/si-MUC5AC cells showed weak expression of TRAIL receptors (DR4/TRAIL-R1 and DR5/TRAIL-R2) and active-caspase 3 and strong expression of pro-caspase 3 (active-caspase 3 precursor). The same expression patterns were observed for SW1990/si-mock cells. However, the addition of TRAIL induced an enhancement in the expression of DR4/TRAIL-R1 and DR5/TRAIL-R2 in SW1990/si-MUC5AC cells. Additionally, a significant increase in active-caspase 3 expression was observed. On the other hand, TRAIL had no effect on DR4/TRAIL-R1 and DR5/TRAIL-R2 expressions in SW1990/si-mock cells.

## Discussion

Mucins are classified generally into two groups: a secretory type and membrane-bound type. Secretory mucins include MUC2, MUC5AC, MUC5B and MUC6. These mucins are called 11p15.5 mucin because they are located on human chromosome 11p15.5 and are structurally similar. On the other hand, membrane-bound mucins include MUC1, MUC3A, MUC3B, MUC4, MUC11, MUC12 and MUC13. All these mucins have transmembrane domains. MUC3A, MUC3B, MUC11 and MUC12 are located on chromosome 7q22, while MUC4 and MUC13 are located on chromosome 3q29. MUC7 and MUC8 belong to neither of the above groups and have no mutual similarity (3,14). The core protein of a mucin molecule has a characteristic repetitive sequence. The repetitive sequence, rich in Thr and Ser, is frequently bound to a mucin-type sugar chain. Mucin-type sugar chains generally consist of N-acetylgalactosamine, N-acetylglucosamine, galactose, fucose and sialic acid. Sugar chains account for 50-80% or above of the molecular weight of mucin, giving it various properties including viscosity, a water-holding capacity and proteinase resistance. Thus, the sugar chain structure of mucin, which is varied quantitatively and qualitatively with malignant transformations, is likely to be involved in altered adhesion during metastasis and evasion from immune cells. However, the detailed mechanisms remain unclear.

We established MUC5AC-knockdown cells using siRNA and have previously reported analysis of the functions of MUC5AC in cancer cells (12). A stable human pancreatic cancer cell line, SW1990/si-MUC5AC, obtained by introducing si-MUC5AC into a parent SW1990, was almost equal to the control cells, SW1990/si-mock, regarding *in vitro* morphology, proliferation and infiltration capacity. However, an *in vivo* subcutaneously implanted model yielded results completely different between SW1990/si-MUC5AC and SW1990/si-mock cells. SW1990/si-mock cells caused continuous rapid tumor growth, whereas SW1990/si-MUC5AC cells caused only slight tumor growth when they were subcutaneously implanted into nude mice. Furthermore, the amounts of immune cells, including neutrophils and B cells, existed in the tumor derived from SW1990/si-MUC5AC cells. Tumor-specific antibodies also existed in the serum. This suggests that MUC5AC-expressing cells may suppress immune cells to evade the immune system, thereby playing an important role in creating an environment to facilitate cancer cell survival.

Neutrophils are characterized by immunity against bacteria, such as direct phagocytosis of bacteria and opsonophagocytosis of encapsulated bacteria. According to previous reports, neutrophils also have antitumor effects. The antitumor effects of neutrophils are reportedly caused by a number of mechanisms including ADCC activity through a tumor-specific antibody, apoptosis induction mediated by TRAIL (15-19). Furthermore, inhibition of tumor growth by IL-12 was reduced when neutrophils were depleted in a mouse model of prostate cancer (20). PMNs are the predominant effector cell population for the killing of breast cancer cells in the presence of HER-2/neu monoclonal antibody (6). In addition, PMN-mediated ADCC has been reported to contribute to the efficacy of the antitumoral antibody rituximab and trastuzumab (13,21,22).

Additionally, TRAIL is expressed at significantly higher levels in neutrophils than in other immune cells. TRAIL was isolated in 1995 as a cytokine that induces apoptosis and has a TNF-family analogous sequence (23). TRAIL is ~30 kDa type II cell surface protein consisting of 281 amino acids and is

about 28% homologous to the Fas ligand. TRAIL induces apoptosis in various malignant tumors, but is non-toxic to normal cells. These functions of TRAIL may lead to the promise of a molecular target agent. TRAIL receptors are classified into TRAIL-R1 (death receptor 4, DR4); TRAIL-R2 (death receptor 5, DR5); TRAIL-R3 (decoy receptor 1, DcR1); TRAIL-R4 (decoy receptor 2, DcR2) and osteoprotegerin (OPG). DRs 4 and 5 have an intracellular death domain to induce apoptosis through initiator and effector caspases, whereas DcRs 1 and 2 are decoy receptors that do not induce apoptosis (10). Differences in TRAIL receptor expressions possibly result in apoptosis induction only in malignant tumors. However, its detailed mechanism remains unclear.

The present study aimed to identify the immune cells on which MUC5AC acts using an immune cell-depleted animal model and analyze the suppression mechanism. Then, we investigated the tumor growth of MUC5AC-knockdown cells using nude mice depleted of neutrophils with an anti-Gr-1 antibody and SCID mice depleted of B and T cells.

To examine whether B cells act directly on the rejection of implanted MUC5AC-knockdown cells, we investigated the tumor growth of MUC5AC-knockdown and MUC5AC-expressing cells in SCID mice. The growth of MUC5AC-knockdown cells did not recover (Fig. 1A). In SCID mice, an investigation in the double implantation system demonstrated that the tumor growth of MUC5AC-expressing cells was increased irrespective of whether a primary tumor was present or absent (unpublished observation). However, such growth was not observed in nude mice (unpublished observation). This suggests that MUC5AC suppresses memory B-cell immune reactions that function during prolonged antitumor reactions or cell metastasis.

In an experiment with neutrophil-depleted model mice, the tumor growth of MUC5AC-knockdown cells, barely observed in the presence of neutrophils, was recovered to the same level as MUC5AC-expressing cells when neutrophils were depleted (Fig. 1C). This suggests that MUC5AC plays an important role in directly suppressing the antitumor effects of neutrophils. Additionally, IL-8 production, barely observed in MUC5AC-expressing cells, was significantly increased in MUC5AC-knockdown cells (Fig. 2). According to these results, neutrophil infiltration into a tumor inducing by IL-8 was found to exert antitumor effects. However, the mechanism by which MUC5AC-knockdown increases IL-8 production by tumor cells still remains unknown and should be investigated in a future study.

An apoptosis array was employed to examine why MUC5AC-expressing cells differed from MUC5AC-knockdown cells in their susceptibilities to apoptosis mediated by TRAIL. DR4/TRAIL-R1 and DR5/TRAIL-R2 were weakly expressed in the routine cultures of both cells. However, the addition of TRAIL increased the expressions of DR4/TRAIL-R1, DR5/TRAIL-R2 and active-caspase 3 (effector caspase) in MUC5AC-knockdown cells (Fig. 4). Future studies will be aimed at investigating how TRAIL increases death receptor expressions in MUC5AC-knockdown cells.

The caspase family of proteases is the ultimate effector of programmed cell death. Under ordinary circumstances, caspases are kept in check by the inhibitor of apoptosis proteins (IAPs) such as cIAP1, cIAP2, XIAP, NAIP, livin/ML-IAP, BRUCE/Apollon and survivin, which bind to and inactive caspases until they are needed. Caspases are overexpressed in tumors, but IAPs likewise are overexpressed. Therefore, failure to activate caspases could create resistance to apoptosis (24,25). Several studies show that MUC4 and ErbB2 are coexpressed in some tumor types such as the breast, non-small cell lung cancer, and pancreas. The possibility that MUC4 could elicit its anti-apoptotic effects by ErbB2, engaging a variety of signaling cascades to elicit cellular responses, such as proliferation and survival, has been suggested (26,27). Prostaglandin $E_2$ ($PGE_2$) synthesized by cyclooxygenase-2 (COX-2), overproduced in various malignancies, has also been reported to be associated with anti-apoptotic effects and increase survivin expression (28,29). It is believed that MUC5AC may have promoted the expression or action of IAPs in some way or MUC5AC may have formed a complex with a certain molecule and promoted tumor growth via suppression of tumor cell apoptosis.

In the present study, we established MUC5AC-knockdown cells using siRNA to elucidate the functions of MUC5AC, whose expression is increased in pancreatic cancer. IL-8 production was promoted in MUC5AC-knockdown cells. In addition, cell death was induced by TRAIL through the apoptosis pathway, suggesting reduced tumorigenicity *in vivo*. It was suggested that induction of neutrophil migration is weak in normal MUC5AC-producing pancreatic cancer cells because IL-8 production is low and apoptosis induction by neutrophil-derived TRAIL is blocked due to the presence of MUC5AC, and these conditions promote pancreatic cancer cell proliferation and growth *in vivo*, being involved in aggressive tumor formation. Our observations suggest that the very potent anti-apoptotic effects of MUC5AC allow tumor cells to escape key barriers to tumor progression. These studies add to the knowledge on the significance of MUC5AC expression in cancer cells.

## Acknowledgements

This study was conducted at Kureha Corporation, Tokyo and Osaka City University, Osaka, Japan. Hirotaka Hoshi, Motoyuki Uchida and Hiroko Iijima are employees of Kureha Corporation, but the study presents no conflict of interest.

## References

1. Wang Z, Song W, Aboukameel A, Mohammad M, Wang G, Banerjee S, Kong D, Wang S, Sarkar FH and Mohammad RM: TW-37, a small-molecule inhibitor of Bcl-2, inhibits cell growth and invasion in pancreatic cancer. Int J Cancer 123: 958-966, 2008.
2. Sheehan JK, Brazeau C, Kutay S, Pigeon H, Kirkham S, Howard M and Thornton DJ: Physical characterization of the MUC5AC mucin: a highly oligomeric glycoprotein whether isolated from cell culture or in vivo from respiratory mucous secretions. Biochem J 347: 37-44, 2000.
3. Hollingsworth MA and Swanson BJ: Mucins in cancer: protection and control of the cell surface. Nat Rev Cancer 4: 45-60, 2004.
4. Ho JJL, Crawley S, Pan PL, Farrelly ER and Kim YS: Secretion of MUC5AC mucin from pancreatic cancer cells in response to forskolin and VIP. Biochem Biophys Res Commun 294: 680-686, 2002.
5. Tecchio C, Huber V, Scapini P, Calzetti F, Margotto D, Todeschini G, Pilla L, Martinelli G, Pizzolo G, Rivoltini L and Cassatella MA: IFNalpha-stimulated neutrophils and monocytes release a soluble form of TNF-related apoptosis-inducing ligand (TRAIL/Apo-2 ligand) displaying apoptotic activity on leukemic cells. Blood 103: 3837-3844, 2004.